Eigenmodes for capillary tubes with dielectric walls and ultraintense laser pulse guiding

B. Cros, C. Courtois, and G. Matthieussent
LPGP, CNRS UMR 8578, Université Paris XI, Bâtiment 210, 91405 Orsay cedex, France

A. Di Bernardo and D. Batani
Dipartimento di Fisica, Università degli Studi Milano–Bicocca, Milano, Italy

N. Andreev and S. Kuznetsov
Institute for High Energy Densities, Associated Institute for High Temperatures of RAS, Izhorskaya 13/19, Moscow 127412, Russia
(Received 5 June 2001; published 24 January 2002)

The properties of the eigenmodes of a capillary tube are examined in the context of ultrashort intense laser pulse guiding. The dispersion relation for the eigenmodes of a cylindrical hollow waveguide is derived and the family of eigenmodes $EH_{\nu s}$ is shown to be a solution of the wave equation up to the first order under the condition $k_0 a \gg 1$, where k_0 is the light wave number and a the capillary tube radius. The expressions of the fields for the eigenmodes are given at zero and first order of a small parameter equal to the ratio of the perpendicular to longitudinal wave number and the absorded intensity at the wall is estimated.

DOI: 10.1103/PhysRevE.65.026405 PACS number(s): 42.79.Gn, 52.38.-r

I. INTRODUCTION

The future development of applications of short pulse, intense lasers such as plasma accelerators [1,2] or x-ray lasers [3,4], relies on the possibility of guiding the laser beam on a distance much larger than the Rayleigh length while maintaining intensities in the range 10^{14} to 10^{19} W/ cm^2. A hollow capillary tube with dielectric walls, used as a leaky guide, makes possible the propagation of ultraintense laser beams on a length of the order of 10 cm. Monomode guiding on the fundamental mode is particularly interesting as it is characterized by a high group velocity, a smooth transverse profile, and a small attenuation factor. A long scale plasma can be created by the guided laser pulse, ionizing a gas filling the capillary tube [5].

In this context, while experiments have been carried out at high intensity in multimode [6,7] or monomode regime [5], there is, to our knowledge, a lack of theoretical work since the early work of Marcatili and Schmeltzer [8]. In particular, it is important, for high intensity propagation to determine (i) the configuration of the mode (spatial dependence of the fields and polarization), (ii) the coupling of the incident laser beam to the eigenmodes of the capillary tube, (iii) the fraction of the maximum intensity absorded at the inner wall of the capillary tube. This value will determine the threshold of incident intensity for plasma formation from the wall of the capillary tube, resulting in a different regime of damping along the propagation after the creation of a plasma wall.

The aim of this paper is to complement the mode analysis that was carried out by Marcatili and Schmeltzer in the context of laser pulse guiding for long distance transmission [8,9]. In particular, the conditions of continuity of the electromagnetic fields and of the flux of the Poynting vector have been checked out at the inner surface of the capillary tube wall. This analysis can be applied to metallic or dielectric capillary tubes by considering the proper dielectric constant of the wall material. It can also be extended to the eigenmodes of a capillary tube filled with a low density homogeneous plasma. In Sec. II, the general dispersion relation for eigenmodes inside a circular waveguide is recalled and its solutions are shown to generate several families of modes. In practice, most of the laser beams exhibit in free space a transverse profile that is a Gaussian function, the usual TEM_{00} mode. Such an incident beam will be predominantly coupled to the so-called EH_{1s} family of hybrid modes. The expression of the fields for the hybrid modes $EH_{\nu s}$ is given in Sec. III, at first order of a small parameter equal to the ratio of the perpendicular to longitudinal wave numbers, and the absorbed intensity at the wall is estimated. The properties of the EH_{1s} modes are examined in Sec. IV.

II. DISPERSION RELATION

The solutions of Maxwell's equations are derived in a cylindrical waveguide of radius a. The wall of the waveguide is assumed to be characterized by a relative dielectric constant ε equal to 1 for $r \leqslant a$, and ε_w for $r \geqslant a$ (Fig. 1). ε_w depends on the material constituting the walls, which can be either dielectric or metallic. The permeability is assumed to be equal to the permeability of free space, μ_0, in both media.

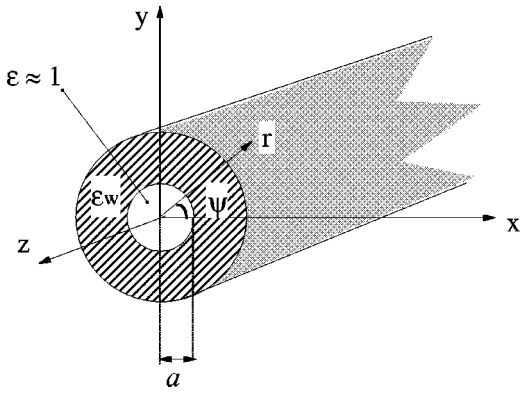

FIG. 1. Notations for cylindrical geometry and dielectric constants.

For oscillating electromagnetic fields with a dependence $e^{i\omega t}$, Maxwell's equations can be written as

$$\vec{\nabla}\wedge\vec{E}=-i\omega\vec{B},\quad \vec{\nabla}\cdot\vec{E}=0, \tag{2.1}$$

$$\vec{\nabla}\wedge\vec{B}=i\omega\varepsilon\vec{E}/c^2,\quad \vec{\nabla}\cdot\vec{B}=0, \tag{2.2}$$

leading, for a constant dielectric fonction to the wave equation for $\vec{B}$ (or $\vec{E}$),

$$\vec{\nabla}^2\vec{B}+k_0^2\varepsilon\vec{B}=0, \tag{2.3}$$

where $k_0=\omega/c$ is the free space wave number in vacuum. We look for a solution of Eq. (2.3) in cylindrical coordinates (Fig. 1)

$$\partial_{r^2}^2 B_z+\frac{1}{r}\partial_r B_z+\frac{1}{r^2}\partial_{\psi^2}^2 B_z+\partial_{z^2}^2 B_z+k_0^2\varepsilon B_z=0. \tag{2.4}$$

For a component of the field along the direction of propagation, B_z, of the form

$$B_z=B_z(r)e^{i(\nu\psi+\omega t-k_z z)},$$

Eq. (2.4) becomes

$$\partial_{r^2}^2 B_z(r)+\frac{1}{r}\partial_r B_z(r)+\left(k_0^2\varepsilon-k_z^2-\frac{\nu^2}{r^2}\right)B_z(r)=0. \tag{2.5}$$

Assuming the boundary conditions $\lim_{r\to\infty}B_z(r)=0$ and $\lim_{r\to\infty}E_z(r)=0$ one obtains the following solutions, for $r\leqslant a$: $\varepsilon\simeq 1$, the dimensionless perpendicular wave number inside the capillary tube, u, is defined as $u^2=a^2(k_0^2-k_z^2)$, and the solutions of Eq. (2.5) are of the form

$$E_z(r)=AJ_\nu\left(u\frac{r}{a}\right), \tag{2.6}$$

$$B_z(r)=BJ_\nu\left(u\frac{r}{a}\right), \tag{2.7}$$

for $r\geqslant a$: $\varepsilon=\varepsilon_w$, is the dielectric constant inside the capillary tube wall, and the perpendicular wave number inside the wall, v, is defined as $v^2=a^2(k_z^2-k_0^2\varepsilon_w)$, giving the solutions

$$E_z(r)=CK_\nu\left(v\frac{r}{a}\right), \tag{2.8}$$

$$B_z(r)=DK_\nu\left(v\frac{r}{a}\right), \tag{2.9}$$

where A, B, C, and D are constants to be determined and J_ν, K_ν are Bessel functions of integer order. It should be noted that a combination of J_ν and Y_ν functions of real argument is also a solution for $r\geqslant a$: the K_ν function has been chosen for convenience.

The other components of the fields are obtained from Maxwell's equations as functions of $E_z(r)$ and $B_z(r)$,

$$E_r(r)=\frac{1}{k_0^2\varepsilon-k_z^2}\left[-ik_z\partial_r E_z(r)+\frac{\omega\nu}{r}B_z(r)\right], \tag{2.10}$$

$$B_r(r)=\frac{1}{k_0^2\varepsilon-k_z^2}\left[-ik_z\partial_r B_z(r)-\frac{\nu k_0^2\varepsilon}{r\omega}E_z(r)\right], \tag{2.11}$$

$$E_\psi(r)=\frac{1}{k_0^2\varepsilon-k_z^2}\left[i\omega\partial_r B_z(r)+\frac{k_z\nu}{r}E_z(r)\right], \tag{2.12}$$

$$B_\psi(r)=\frac{1}{k_0^2\varepsilon-k_z^2}\left[-i\frac{k_0^2\varepsilon}{\omega}\partial_r E_z(r)+\frac{k_z\nu}{r}B_z(r)\right]. \tag{2.13}$$

Expressing the continuity of the components εE_r, E_z, E_ψ, B_z, B_r, and B_ψ at the boundary $r=a$, one gets

$$C=A\frac{J_\nu(u)}{K_\nu(v)}, \tag{2.14}$$

$$D=B\frac{J_\nu(u)}{K_\nu(v)}, \tag{2.15}$$

$$B=iA\nu\frac{k_z}{\omega}\left(\frac{1}{u^2}+\frac{1}{v^2}\right)\left(\frac{1}{u}\frac{J_\nu'(u)}{J_\nu(u)}+\frac{1}{v}\frac{K_\nu'(v)}{K_\nu(v)}\right)^{-1}, \tag{2.16}$$

and the dispersion relation [8,9]

$$k_z^2\nu^2\left(\frac{1}{u^2}+\frac{1}{v^2}\right)^2=\left(\frac{1}{u}\frac{J_\nu'(u)}{J_\nu(u)}+\frac{1}{v}\frac{K_\nu'(v)}{K_\nu(v)}\right)\left(\frac{k_0^2}{u}\frac{J_\nu'(u)}{J_\nu(u)}+\frac{k_0^2\varepsilon_w}{v}\frac{K_\nu'(v)}{K_\nu(v)}\right), \tag{2.17}$$

where the prime denotes the derivative with respect to the argument of the functions.

The dispersion relation can be solved analytically under the condition $k_0 a\gg 1$, i.e., for incident laser beam wavelengths much smaller than the inner capillary tube radius. This condition leads to $k_z\simeq k_0$, $|v|\gg 1$, $|u/v|\ll 1$, and the asymptotic expressions for large arguments of the K_ν functions and their derivatives can be used.

A. Transverse modes: $\nu=0$

For $\nu=0$, the dispersion relation Eq. (2.17), splits into two relations, for which one term of the right-hand side is equal to zero.

The first relation is

$$\frac{J_0'(u)}{J_0(u)}=-\frac{u}{v}\frac{K_0'(v)}{K_0(v)}. \tag{2.18}$$

With this condition, the constant B will have a finite value for $A=0$, which implies $C=0$ and $E_z(r)=0$. These modes are the so-called transverse electric or TE_{0s} modes; the index

s indicates that the mode is derived from the sth root of the equation $J_1(u_s)=0$. The normalized field components inside the capillary tube can be expressed as

$$E_z(r)=E_r(r)=B_\psi(r)=0, \tag{2.19}$$

$$E_\psi(r)=-\frac{\omega}{k_z}J_1(ur/a), \tag{2.20}$$

$$B_r(r)=J_1(ur/a), \tag{2.21}$$

$$B_z(r)=-i\frac{u}{k_z a}J_0(ur/a). \tag{2.22}$$

With the assumption $k_z a/u \gg 1$, it follows that $B_r \gg B_z$; the magnetic field is essentially radial, and the electric field is purely azimuthal.

The second relation is

$$\frac{J_0'(u)}{J_0(u)}=-\frac{u\varepsilon_w}{v}\frac{K_0'(v)}{K_0(v)}, \tag{2.23}$$

which implies $B=D=0$ and $B_z(r)=0$. These modes are the so-called transverse magnetic or TM_{0s} modes. The normalized field components inside the capillary tube can be expressed as

$$E_\psi(r)=B_z(r)=B_r(r)=0, \tag{2.24}$$

$$E_z(r)=-i\frac{u}{k_z a}J_0(ur/a), \tag{2.25}$$

$$E_r(r)=J_1(ur/a), \tag{2.26}$$

$$B_\psi(r)=\frac{k_z}{\omega}J_1(ur/a). \tag{2.27}$$

Here, the electric field is mainly radial and the magnetic field purely azimuthal.

These TE or TM modes are not appropriate for coupling an incident Gaussian beam with linear polarization. In both cases, the transverse polarization is not linear so that the energy of the incident beam cannot be coupled to these modes. Other modes more similar to the Gaussian profile of the laser beam have to be looked for in order to insure coupling.

B. Hybrid modes: $\nu \neq 0$

In this section, analytical solutions of the dispersion relation are derived in the general case $\nu \neq 0$. For large $|v|$,

$$K_\nu'(v) \simeq -K_\nu(v), \tag{2.28}$$

and with the condition $k_0 a \gg 1$, which leads to $|u/v| \ll 1$, the dispersion relation (2.17) is approximated for $\nu \neq 0$ as

$$\left(\frac{J_\nu'(u)}{J_\nu(u)}-\frac{u}{v}\right)\left(\frac{J_\nu'(u)}{J_\nu(u)}-\frac{u\varepsilon_w}{v}\right)\sim\frac{\nu^2}{u^2}. \tag{2.29}$$

Using the recurrence relation

$$\frac{J_\nu'(u)}{J_\nu(u)}=\frac{J_{\nu-1}(u)}{J_\nu(u)}-\frac{\nu}{u}, \tag{2.30}$$

and neglecting small terms of order 2 or higher in u/v, one gets a simplified form of the dispersion relation

$$\frac{J_{\nu-1}(u)}{J_\nu(u)}\sim\frac{\nu}{u}+\frac{u}{2v}(1+\varepsilon_w)\pm\frac{\nu}{u}. \tag{2.31}$$

In the above relation, the positive sign corresponds, for small values of u, to large values of the ratio $J_{\nu-1}(u)/J_\nu(u)$ and the equation does not have any solution. So the dispersion relation is finally

$$J_{\nu-1}(u)\sim\frac{u}{2v}(1+\varepsilon_w)J_\nu(u). \tag{2.32}$$

As u/v is a small parameter we look for a solution u of Eq. (2.32) such that $J_{\nu-1}(u)\sim 0$; writing $u=u_s+\Delta u$, with u_s such that $J_{\nu-1}(u_s)=0$, and Δu small, one gets

$$\begin{aligned}J_{\nu-1}(u_s+\Delta u)&\simeq J_{\nu-1}(u_s)+\Delta u J_{\nu-1}'(u_s)\\&\simeq\Delta u\left(J_{\nu-2}(u_s)-\frac{\nu}{u_s}J_{\nu-1}(u_s)\right)\\&\simeq\Delta u J_{\nu-2}(u_s),\end{aligned}$$

and with $J_\nu(u_s)=-J_{\nu-2}(u_s)$,

$$\Delta u=-\frac{u_s}{2k_0 a}\frac{1+\varepsilon_w}{\sqrt{1-\varepsilon_w}}. \tag{2.33}$$

The longitudinal wave vector is retrieved from the assumption $k_z=k_{z0}+\delta k$, with δk a complex number such that $|\delta k/k_{z0}| \ll 1$ and k_{z0} such that $u_s^2=a^2(k_0^2-k_{z0}^2)$. Differentiating the previous expression leads to

$$\delta k=-\frac{u_s}{k_{z0}a^2}\Delta u,$$

or

$$\delta k=\frac{u_s^2}{2k_{z0}^2a^3}\frac{1+\varepsilon_w}{\sqrt{1-\varepsilon_w}}. \tag{2.34}$$

The imaginary part of δk, k_{zi}, is the damping factor for the propagation of the fields along the z axis. It is strongly dependent on the capillary tube radius, on the wavelength of the incident beam, and on the mode order through u_s.

This damping is due to refraction losses in the dielectric walls and occurs for a real dielectric constant when $\varepsilon_w > 1$, so that

$$k_{zi}=-\frac{u_s^2}{2k_{z0}^2a^3}\frac{1+\varepsilon_w}{\sqrt{\varepsilon_w-1}}.$$

A characteristic damping length, L_d, is associated to the inverse of $|k_{zi}|$. L_d is the propagation length after which the fields amplitude is divided by e. For the case of glass walls ($\varepsilon_w=2.25$), an incident wavelength of 1 μm and a capillary tube radius $a=25$ μm, $L_d=7.3$ cm for the less damped mode with $\nu=1$ and $u_s=2.4$.

The dispersion relation can be written in the familiar form $\omega^2 \simeq c^2(k_z^2+k_{\perp s}^2)$ with $k_z \sim k_0$ and $k_{\perp s}=u_s/a$. The group velocity is $v_{gs} \simeq c(1-k_{\perp s}^2/k_0^2)^{1/2}$, close to the velocity of light in free space under the hypothesis made, $k_{\perp s} \ll k_0$. Note that the group velocity decreases as the mode order s increases.

In order to obtain the expression for the field components, one also needs to express the constant B, given by Eq. (2.16) at order 1 of the small parameter u/v. Using Eq. (2.28) and the dispersion relation (2.32), the expression of B becomes

$$B \simeq iA\frac{k_z}{\omega}\nu\left(\frac{1}{u^2}+\frac{1}{v^2}\right)\left[\frac{1}{u}\left(\frac{u}{2v}(1+\varepsilon_w)-\frac{\nu}{u}\right)-\frac{1}{v}\right]^{-1},$$

so that

$$B \simeq -iA\frac{k_z}{\omega}\frac{1+u^2/v^2}{\left(1+\dfrac{u^2}{2\nu v}(1-\varepsilon_w)\right)},$$

and finally at first order in u/v,

$$B \simeq -iA\frac{k_z}{\omega}\left(1-\frac{u^2}{2\nu v}(1-\varepsilon_w)\right). \tag{2.35}$$

III. PROPERTIES OF HYBRID MODES

As will be shown in Sec. IV, an incident Gaussian beam can be coupled efficiently to some of the hybrid modes. Therefore, the rest of the paper will focus on the properties of these modes. In order to simplify the presentation, the expression of the fields will be given for the case of dielectric walls, for which the dielectric constant is real and larger than unity. However, it should be noted that the results for the case of metallic walls are retrieved by performing a similar analysis.

The components of the transverse fields are retrieved by inserting the solutions (2.6) and (2.7) for $r \leqslant a$ [Eqs. (2.8) and (2.9) for $r \geqslant a$], into Eqs. (2.10) to (2.13), with the expression of the constant B given by Eq. (2.35). The field components are functions of the small parameter u/v and of $J_\nu(ur/a)$ and $J_{\nu-1}(ur/a)$ for $r \leqslant a$[$K_\nu(vr/a)$ and $K_{\nu-1}(vr/a)$ for $r \geqslant a$].

In order to obtain the expressions of the fields at first order in u/v, valid for all $r \leqslant a$ including at the boundary $r=a$, the Bessel functions $J_\nu(ur/a)$ and $J_{\nu-1}(ur/a)$ are developed using the Taylor's formula for $u=u_s+\Delta u$, with $\Delta u=-u_s(1+\varepsilon_w)/(2v)$. Using the following developments:

$$J_{\nu-1}\left(u\frac{r}{a}\right)=J_{\nu-1}\left(u_s\frac{r}{a}\right)\left[1+\frac{(\nu-1)\Delta u}{u_s}\right]-\Delta u\frac{r}{a}J_\nu\left(u_s\frac{r}{a}\right),$$

$$J_\nu\left(u\frac{r}{a}\right)=J_\nu\left(u_s\frac{r}{a}\right)\left[1-\frac{\nu\Delta u}{u_s}\right]+\Delta u\frac{r}{a}J_{\nu-1}\left(u_s\frac{r}{a}\right),$$

and neglecting terms of order $1/v^2$, the real part of the fields for $r \leqslant a$ can be expressed as

$$E_{z\pm}=\pm\frac{k_{\perp s}}{k_{z0}}J_\nu(k_{\perp s}r)\cos(\phi_\pm)e^{k_{zi}z}, \tag{3.1}$$

$$B_{z\pm}=\pm\frac{k_{z0}}{\omega}\frac{k_{\perp s}}{k_{z0}}J_\nu(k_{\perp s}r)\sin(\phi_\pm)e^{k_{zi}z}, \tag{3.2}$$

$$E_{r\pm}=\left\{J_{\nu-1}(k_{\perp s}r)\sin(\phi_\pm)\mp\frac{k_{\perp s}}{2k_0}\left[\left(\eta\frac{r}{a}+\beta\frac{a}{r}\right)J_\nu(k_{\perp s}r)+\eta\frac{(2-\nu)}{k_{\perp s}a}J_{\nu-1}(k_{\perp s}r)\right]\cos(\phi_\pm)\right\}e^{k_{zi}z}, \tag{3.3}$$

$$E_{\psi\pm}=\left\{J_{\nu-1}(k_{\perp s}r)\cos(\phi_\pm)\pm\frac{k_{\perp s}}{2k_0}\left[\left(\eta\frac{r}{a}-\beta\frac{a}{r}\right)J_\nu(k_{\perp s}r)+\left(\eta\frac{(2-\nu)}{k_{\perp s}a}+\beta\frac{k_{\perp s}a}{\nu}\right)J_{\nu-1}(k_{\perp s}r)\right]\sin(\phi_\pm)\right\}e^{k_{zi}z}, \tag{3.4}$$

$$B_{r\pm}=-\frac{k_{z0}}{\omega}E_{\psi\pm}, \tag{3.5}$$

$$B_{\psi\pm}=\frac{k_{z0}}{\omega}E_{r\pm}, \tag{3.6}$$

where $k_{\perp s}=u_s/a$, is the perpendicular wave vector associated to the root u_s, and the coefficients η and β are defined as $\beta=(\varepsilon_w-1)^{1/2}$, $\eta=(1+\varepsilon_w)/\beta$; $\phi_\pm=\nu\psi\pm(\omega t-k_{z0}z)$. The $\pm$ signs correspond to two solutions: the ϕ_+ solution has been derived in Sec. II. The ϕ_- solution is obtained in a similar way after changing ω into $-\omega$, k_z into $-k_z^\star$, where $\star$ denotes the complex conjugate, and $E_z(r)$ $[B_z(r)]$ into $-E_z(r)$ $[-B_z(r)]$. For both solutions, the transverse components of the fields are much larger than the longitudinal components under the assumption $k_0a \gg 1$, so that these modes are quasitransverse; they are circularly polarized at zero order in $k_{\perp s}/k_0$; at first order the polarization is elliptic. These modes are of interest for the coupling of incident circularly polarized Gaussian beams to the capillary tube: for $\nu=1$, the energy repartition of the Bessel function J_0 is similar to the one of a Gaussian function.

For $r \geqslant a$, the asymptotic expansions of the K_ν Bessel functions for large arguments are used, giving for the real part of the fields

$$E_{z\pm}=\pm\frac{k_{\perp s}}{k_{z0}}J_\nu(k_{\perp s}a)\sqrt{\frac{a}{r}}\cos[\phi_\pm\mp k_{z0}\beta(r-a)]e^{k_{zi}z}, \tag{3.7}$$

$$B_{z\pm}=\pm\frac{k_{z0}}{\omega}\frac{k_{\perp s}}{k_{z0}}J_\nu(k_{\perp s}a)\sqrt{\frac{a}{r}}\sin[\phi_\pm\mp k_{z0}\beta(r-a)]e^{k_{zi}z}, \tag{3.8}$$

$$E_{r\pm}=\mp\frac{k_{\perp s}}{k_{z0}\beta}J_\nu(k_{\perp s}a)\sqrt{\frac{a}{r}}\cos[\phi_\pm\mp k_{z0}\beta(r-a)]e^{k_{zi}z}, \tag{3.9}$$

$$E_{\psi\pm}=\pm\frac{k_{\perp s}}{k_{z0}\beta}J_\nu(k_{\perp s}a)\sqrt{\frac{a}{r}}\sin[\phi_\pm\mp k_{z0}\beta(r-a)]e^{k_{zi}z}, \tag{3.10}$$

$$B_{r\pm}=-\frac{k_{z0}}{\omega}E_{\psi\pm}, \tag{3.11}$$

$$B_{\psi\pm}=\varepsilon_w\frac{k_{z0}}{\omega}E_{r\pm}. \tag{3.12}$$

Writing the Eqs. (3.1)–(3.6) and (3.7)–(3.12) for $r=a$, the continuity of εE_r and the other field components is easily checked.

The intensity lost at the boundary $r=a$ is obtained from the expression of the real part of the radial component of the Poynting vector, averaged over one period and computed for $r=a$,

$$S_r(a)=\frac{1}{\mu_0}(E_\psi B_z-E_z B_\psi)_{r=a}, \tag{3.13}$$

$$S_r(a)=\varepsilon_0 c\frac{k_{\perp s}^2}{k_0^2}J_\nu^2(k_{\perp s}a)\frac{1+\varepsilon_w}{\sqrt{\varepsilon_w-1}}e^{2k_{zi}z}. \tag{3.14}$$

For these circularly polarized modes, the intensity lost at the boundary $r=a$ is independent of the azimuthal angle ψ. Thus the energy of the beam can be deposited homogeneously at the surface of the wall, which is an interesting property for plasma creation from wall ionization.

IV. MONOMODE GUIDING

In practice, the main case of interest for the experiments is to couple the incident energy of a linearly polarized, Gaussian laser beam to eigenmodes of the capillary tube. The incident energy will in that case be coupled efficiently to linearly polarized modes. A linearly polarized family of hybrid modes, the EH_{1s} modes, can be obtained by linear combination of the two solutions presented in Sec. III. The coupling coefficient, defined as the fraction of the incident energy coupled to a set of eigenmodes, can be computed analytically for a linearly polarized incident Gaussian beam. Due to the orthogonality properties of the Bessel functions and to the linear polarization of the incident beam, the coupling coefficient is different from zero only for eigenmodes with $\nu=1$, i.e., the EH_{1s} modes. In addition, it has been shown [10] that the EH_{11} mode can be selected by adjusting the waist w_0 of the incident Gaussian beam at the entrance of the capillary tube: for $w_0=0.645a$, 98% of the incident energy is coupled to the EH_{11} mode, leading to monomode propagation. In this section, the properties of the EH_{1s} modes will then be presented in detail.

A. Field components

The field components of the $EH_{\nu s}$ modes are derived from linear combinations of the type $N_n=(N_{n+}+N_{n-})/2$, where N stands for E or B and $n=z$, r, or ψ; they can be written for $r\leqslant a$ as

$$E_z=-\frac{k_{\perp s}}{k_{z0}}J_\nu(k_{\perp s}r)\sin(\nu\psi)\sin(\omega t-k_{z0}z)e^{k_{zi}z}, \tag{4.1}$$

$$B_z=\frac{k_{z0}}{\omega}\frac{k_{\perp s}}{k_{z0}}J_\nu(k_{\perp s}r)\cos(\nu\psi)\sin(\omega t-k_{z0}z)e^{k_{zi}z}, \tag{4.2}$$

$$\begin{aligned}E_r=\Bigg\{&J_{\nu-1}(k_{\perp s}r)\sin(\nu\psi)\cos(\omega t-k_{z0}z)\\&+\frac{k_{\perp s}}{2k_0}\left[\left(\eta\frac{r}{a}+\beta\frac{a}{r}\right)J_\nu(k_{\perp s}r)+\eta\frac{(2-\nu)}{k_{\perp s}a}J_{\nu-1}(k_{\perp s}r)\right]\\&\times\sin(\nu\psi)\sin(\omega t-k_{z0}z)\Bigg\}e^{k_{zi}z},\end{aligned} \tag{4.3}$$

$$\begin{aligned}E_\psi=\Bigg\{&J_{\nu-1}(k_{\perp s}r)\cos(\nu\psi)\cos(\omega t-k_{z0}z)\\&+\frac{k_{\perp s}}{2k_0}\left[\left(\eta\frac{r}{a}-\beta\frac{a}{r}\right)J_\nu(k_{\perp s}r)\right.\\&\left.+\left(\eta\frac{(2-\nu)}{k_{\perp s}a}+\beta\frac{k_{\perp s}a}{\nu}\right)J_{\nu-1}(k_{\perp s}r)\right]\\&\times\cos(\nu\psi)\sin(\omega t-k_{z0}z)\Bigg\}e^{k_{zi}z},\end{aligned} \tag{4.4}$$

$$B_r=-\frac{k_{z0}}{\omega}E_\psi, \tag{4.5}$$

$$B_\psi=\frac{k_{z0}}{\omega}E_r. \tag{4.6}$$

At zero order in $k_{\perp s}/k_0$, $E_z=B_z=0$, so that this mode is transverse while all the components are of the same order of magnitude at first order.

For $r\geqslant a$, the components are expressed as

$$\begin{aligned}E_z=&-\frac{k_{\perp s}}{k_{z0}}J_\nu(k_{\perp s}a)\sqrt{\frac{a}{r}}\sin(\nu\psi)\\&\times\sin[\omega t-k_{z0}z-k_{z0}\beta(r-a)]e^{k_{zi}z},\end{aligned} \tag{4.7}$$

$$\begin{aligned}B_z=&\frac{k_{z0}}{\omega}\frac{k_{\perp s}}{k_{z0}}J_\nu(k_{\perp s}a)\sqrt{\frac{a}{r}}\cos(\nu\psi)\\&\times\sin[\omega t-k_{z0}z-k_{z0}\beta(r-a)]e^{k_{zi}z},\end{aligned} \tag{4.8}$$

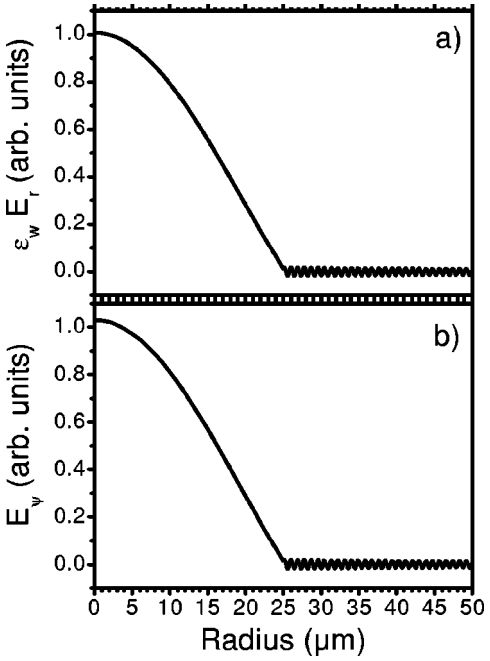

FIG. 2. (a) Radial and (b) azimuthal components of the electric field of the EH_{11} mode as a function of the radial position for $\omega t - k_{z0}z = \psi = \pi/4$, in the case of glass walls ($\varepsilon_w = 2.25$), an incident wavelength of 1 μm and a capillary tube radius $a = 25$ μm.

$$E_r = \frac{k_{\perp s}}{k_{z0}\beta} J_\nu(k_{\perp s}a) \sqrt{\frac{a}{r}} \sin(\nu\psi) \times \sin[\omega t - k_{z0}z - k_{z0}\beta(r-a)] e^{k_{zi}z}, \tag{4.9}$$

$$E_\psi = \frac{k_{\perp s}}{k_{z0}\beta} J_\nu(k_{\perp s}a) \sqrt{\frac{a}{r}} \cos(\nu\psi) \times \sin[\omega t - k_{z0}z - k_{z0}\beta(r-a)] e^{k_{zi}z}, \tag{4.10}$$

$$B_r = -\frac{k_{z0}}{\omega} E_\psi, \tag{4.11}$$

$$B_\psi = \varepsilon_w \frac{k_{z0}}{\omega} E_r. \tag{4.12}$$

These fields satisfy the continuity conditions at the boundary $r = a$ as can be seen in Fig. 2, where $\varepsilon_w E_r$ and E_ψ are plotted as a function of r, for $\nu = 1$, $\omega t - k_{z0}z = \psi = \pi/4$, in the case of glass walls ($\varepsilon_w = 2.25$), an incident wavelength of 1 μm and a capillary tube radius $a = 25$ μm. For $r \leqslant a$, the profile is a J_0 Bessel function while for $r \geqslant a$, the electric fields are slowly damped with a $(r/a)^{-1/2}$ dependence and oscillate with a wavelength equal to λ_0/β.

B. Polarization

Going back to the (x,y) coordinates in the transverse frame, the electric field is transformed as

$$E_x = E_r \cos\psi - E_\psi \sin\psi, \tag{4.13}$$

$$E_y = E_r \sin\psi + E_\psi \cos\psi, \tag{4.14}$$

which gives at zero order for $r \leqslant a$,

$$E_x = J_{\nu-1}(k_{\perp s}r)\sin(\nu-1)\psi \cos(\omega t - k_{z0}z) e^{k_{zi}z}, \tag{4.15}$$

$$E_y = J_{\nu-1}(k_{\perp s}r)\cos(\nu-1)\psi \cos(\omega t - k_{z0}z) e^{k_{zi}z}, \tag{4.16}$$

showing that at zero order, the family of modes given by $\nu = 1$ is linearly polarized. It can be easily checked that the polarization is also linear for $r > a$.

At first order for $r \leqslant a$, however, the polarization is elliptic. The first order terms insure the continuity of the fields at the boundary $r = a$ and cause the bending of the field lines in a layer of thickness $\Delta r \simeq \lambda_0/2\pi$, where the first order terms are larger than the zero order terms $[J_0(k_{\perp s}r) < k_{\perp s}/k_0 \; J_1(k_{\perp s}r)]$.

C. Contrast

The contrast at the capillary tube wall C_w is defined as the ratio of the longitudinal component of the Poynting vector at $r = 0$ to the same component taken at $r = a$; for the EH_{1s} mode, it is given by

$$C_w = \frac{k_0^2}{k_{\perp s}^2 J_1^2(k_{\perp s}a)} \frac{(\varepsilon_w - 1)}{(\cos^2\psi + \varepsilon_w^2 \sin^2\psi)}. \tag{4.17}$$

The contrast grows with the square of $k_0/k_{\perp s}$, which is large under the assumptions made, and decreases with the mode order, as $k_{\perp s}$ grows with s. For glass, with the above parameters ($k_0 a \simeq 157$) and $\psi = 0$, $C_w \simeq 2 \times 10^4 (8.8 \times 10^3)$ for the EH_{11} (EH_{12}) mode.

The normalized flux at the wall F_w is defined as the ratio of the radial component of the Poynting vector at $r = a$ to the the longitudinal component of the Poynting vector at $r = 0$ and is given by

$$F_w = \frac{k_{\perp s}^2}{k_0^2} J_1^2(k_{\perp s}a) \frac{(\cos^2\psi + \varepsilon_w \sin^2\psi)}{(\varepsilon_w - 1)^{1/2}}, \tag{4.18}$$

F_w depends on the azimuthal angle ψ, indicating that the flux deposited at the wall is not homogeneous. F_w is minimum for $\psi = 0, \pi$ and maximum for $\psi = \pi/2, 3\pi/2$.

F_w is used to estimate the maximum intensity that can be guided on a given mode EH_{1s} without ionization of the wall material. In the case of glass, for a pulse duration of the order of 100 fs, the ionization threshold [11] is of the order of 10^{14} W/cm^2 at a wavelength of 0.8 μm. For these parameters and a capillary tube of 25 μm radius, F_w has a maximum value of the order of 10^{-4}. The maximum intensity guided on the fundamental mode EH_{11} without wall ionization is then of the order of 10^{18} W/cm^2.

V. CONCLUSION

In this paper, the dispersion relation for the eigenmodes of a cylindrical, evacuated waveguide has been derived. The

family of hybrid modes $EH_{\nu s}$ is a solution of the wave equation under the assumption $k_0 a \gg 1$. The expressions of the field components have been derived at first order of the small parameter $k_{\perp s}/k_0$ and the continuity at the wall boundary has been checked. The EH_{1s} modes are transverse and linearly polarized at zero order; at first order, the longitudinal component is different from zero (these hybrid modes can be called quasitransverse) and the polarization is elliptic. The analytical estimation of the damping rate along the propagation and of the intensity absorbed at the wall have been given.

The properties of these EH_{1s} modes are such that it is possible to couple efficiently an incident beam in its fundamental Gaussian mode to one of the modes, the fundamental mode EH_{11}. As this mode is characterized with a high group velocity and a large damping length, it is particularly interesting to couple the incident beam to this mode for applications of monomode guiding.

The expressions of the contrast and of the intensity absorbed at the wall allow to estimate the maximum intensity on axis that can be guided without damaging the capillary tube walls. It should be mentioned however, that for ultrashort pulses, this should not be a limitation. Even if a plasma is created at the wall, this plasma does not expand during the pulse duration. The guiding is then performed by the high-density, steep-gradient plasma existing near the wall surface. The estimation of the damping in this case will be the objective of future work.

ACKNOWLEDGMENTS

This work was partly supported by the program FEMTO of the European Science Foundation, by INTAS Project No. 97-10236, and by NATO Collaborative Linkage Grant No. PST. 976812.

[1] T. Tajima and J. M. Dawson, Phys. Rev. Lett. **43**, 267 (1979).
[2] F. Amiranoff, S. Baton, D. Bernard, B. Cros, D. Descamps, F. Dorchies, F. Jacquet, V. Malka, J. R. Marquès, G. Matthieussent, P. Miné, A. Modena, P. Mora, J. Morillo, and Z. Najmudin, Phys. Rev. Lett. **81**, 995 (1998).
[3] H. M. Milchberg, J. Opt. Soc. Am. B **12**, 731 (1995).
[4] A. Y. Goltsov, D. V. Korobkin, YI. Ping, and S. Suckewer, J. Opt. Soc. Am. B **17**, 868 (2000).
[5] F. Dorchies, J. R. Marquès, B. Cros, G. Matthieussent, C. Courtois, T. Vélikoroussov, P. Audebert, J. P. Geindre, S. Rebibo, G. Hamoniaux, and F. Amiranoff, Phys. Rev. Lett. **82**, 4655 (1999).
[6] S. Jackel, R. Burris, J. Grun, A. Ting, C. Manka, K. Evans, and J. Kosakowskii, Opt. Lett. **20**, 1086 (1995).
[7] M. Borghesi, A. J. Mackinnon, R. Gaillard, O. Willi, and A. A. Offenberger, Phys. Rev. E **57**, R4899 (1998).
[8] E. A. J. Marcatili and R. A. Schmeltzer, Bell Syst. Tech. J. **43**, 1783 (1964).
[9] M. J. Adams, *An Introduction to Optical Waveguides* (Wiley, New York, 1981).
[10] R. L. Abrams, IEEE J. Quantum Electron. **QE-8**, 838 (1972).
[11] D. Du, X. Liu, G. Korn, J. Squier, and G. Mourou, Appl. Phys. Lett. **64**, 3071 (1994).